

Transverse momentum spectra of charged hadrons in jets at the Tevatron

Redamy Perez Ramos^{1 a}

II. Institut für Theoretische Physik, Universität Hamburg

Received: date / Revised version: date

Abstract The hadronic k_{\perp} -spectrum inside a high energy jet is determined including corrections of relative magnitude $\mathcal{O}(\sqrt{\alpha_s})$ with respect to the Modified Leading Logarithmic Approximation (MLLA), in the limiting spectrum approximation (assuming an infrared cut-off $Q_0 = \Lambda_{\text{QCD}}$) and beyond ($Q_0 \neq \Lambda_{\text{QCD}}$). The results in the limiting spectrum approximation are found to be, after normalization, in impressive agreement with measurements by the CDF collaboration. A new integral representation for the “hump-backed” plateau is also reported.

PACS. 12.38.-t Quantum chromodynamics – 12.38.Bx Perturbative calculations

1 Introduction

The production of jets – a collimated bunch of hadrons – in e^+e^- , e^-p and hadronic collisions is an ideal playground to investigate the parton evolution process in perturbative QCD (pQCD). One of the great successes of pQCD is the existence of the hump-backed shape of inclusive spectra, predicted in [1] within MLLA, and later discovered experimentally (for review, see e.g. [2]). Refining the comparison of pQCD calculations with jet data taken at LEP, Tevatron and LHC will ultimately allow for a crucial test of the Local Parton Hadron Duality (LPHD) hypothesis [3] and for a better understanding of color neutralization processes.

The inclusive k_{\perp} -distribution of particles inside a jet has been computed at MLLA accuracy in the limiting spectrum approximation [4], *i.e.* assuming an infrared cutoff Q_0 equal to Λ_{QCD} ($\lambda \equiv \ln(Q_0/\Lambda_{\text{QCD}}) = 0$) (for a review, see also [5]). MLLA corrections, of relative magnitude $\mathcal{O}(\sqrt{\alpha_s})$ with respect to the leading double logarithmic approximation (DLA), were shown to be quite substantial [4]. Therefore, it appears legitimate to wonder whether corrections of order $\mathcal{O}(\alpha_s)$, that is next-to-next-to-leading or Next-to-MLLA (NMLLA), are negligible or not.

The starting point of this analysis is the MLLA Master Equation for the *Generating Functional* (GF) $Z = Z(u)$ of QCD jets [5], where $u = u(k)$ is a certain probing function and k , the four-momentum of the outgoing parton. Together with the initial condition at threshold, the GF determines the jet properties at all energies. For instance, the single inclusive spectrum can be derived from the GF by differentiating with respect to $u = u(k)$, and the solution of the equations can be written as a perturbative expansion in $\sqrt{\alpha_s}$. At high energies

this expansion can be resummed and the leading contribution be represented as an exponential of the anomalous dimension $\gamma(\alpha_s)$. Since further details to this logic can be found in [5, 6], we only give the symbolic structure of the equation for the GF and its solution, which we write respectively as

$$\frac{dZ}{dy} \simeq \gamma_0(y)Z \quad \Rightarrow \quad Z \simeq \exp \left\{ \int^y \gamma(\alpha_s(y')) dy' \right\}, \quad (1)$$

where $\gamma(\alpha_s)$ can be expressed as a power series of $\sqrt{\alpha_s}$

$$\gamma(\alpha_s) = \sqrt{\alpha_s} + \alpha_s + \alpha_s^{3/2} + \alpha_s^2 + \dots \quad (2)$$

In this logic, the leading (DLA, $\mathcal{O}(\sqrt{\alpha_s})$) and next-to-leading (MLLA, $\mathcal{O}(\alpha_s)$) approximations are complete. The next terms (NMLLA, $\mathcal{O}(\alpha_s^{3/2})$) are not complete but they include an important contribution which takes into account energy conservation and an improved behavior near threshold. Indeed, some results for such NMLLA terms have been studied previously for global observables and have been found to better account for recoil effects and to drastically affect multi-particle production [7, 8].

The equation in (1) applies to each vertex of the cascade and its solution represents the fact that successive and independent partonic splittings inside the shower, exponentiate with respect to the *evolution-time* parameter $dy = d\Theta/\Theta$, where $\Theta \ll 1$ is the angle between outgoing couples of partons. The choice of y follows from Angular Ordering (AO) in intra-jet cascades. It is indeed the suited variable for describing *time-like* evolution in jets. Thus, Eq. (1) incorporates the Markov chains of sequential angular ordered partonic decays which are singular in Θ and $\gamma(\alpha_s)$ determines the real rate of inclusive quantities growth with energy.

While DLA treats the emission of both particles as independent by keeping track of the first term $\sim \sqrt{\alpha_s}$ in (2) without

Send offprint requests to: Redamy Perez Ramos

^a Luruper Chaussee 149, D-22761 Hamburg, Germany

constraint, the exact solution of the MLLA evolution equation (partially) fulfills the energy conservation in each individual splitting process ($z + (1 - z) = 1$) by incorporating higher order ($\alpha_s^{n/2}$, $n > 1$) terms to the anomalous dimension. Symbolically, the first two analytical steps towards a better account of these corrections in the MLLA, NMLLA evolution, which we further discuss in [9], can be represented in the form

$$\Delta\gamma \simeq \int (\alpha_s + \alpha_s \ell^{-1} \ln z) dz \sim \alpha_s + \alpha_s^{3/2}, \quad (3)$$

where $\ell = \ln(1/x) \sim \alpha_s^{-1/2}$ with $x \ll 1$ (fraction of the jet energy taken away by one hadron), $z \sim 1$ for hard partons splittings such as $g \rightarrow q\bar{q}$... (this is in fact the region where the two partons are strongly correlated).

Energy conservation is particularly important for energetic particles as the remaining phase space is then very limited. On the other hand, a soft particle can be emitted with little impact on energy conservation. Some consequences of this behavior have also been noted in [10]:

- (i) the soft particles follow the features expected from DLA;
- (ii) there is no energy dependence of the soft spectrum;
- (iii) the ratio of soft particles $r = N_g/N_q$ in gluon and quark jets is consistent with the DLA prediction $N_c/C_F = 9/4$ (see the measurement by DELPHI [11]).

The present study makes use of this logic (3) to evaluate NMLLA contributions to the single inclusive k_\perp -distribution. The main results of this work have been published in [9, 12]. Experimentally, the CDF collaboration at the Tevatron reported on k_\perp -distributions of unidentified charged hadrons in jets produced in $p\bar{p}$ collisions at $\sqrt{s} = 1.96$ TeV [13].

2 MLLA evolution equations

We start by writing the MLLA evolution equations for the fragmentation function $D_B^h(x/z, zE\Theta_0, Q_0)$ of a parton B (energy zE and transverse momentum $k_\perp = zE\Theta_0$) into a gluon (represented by a hadron h (energy xE) according to LPHD [3]) inside a jet A of energy E for the process depicted in Fig. 1. As a consequence of angular ordering in parton cascading, par-

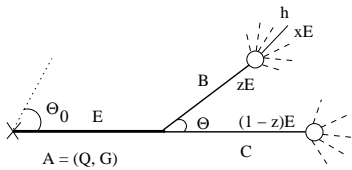


Figure 1. Parton A with energy E splits into parton B (respectively C) with energy zE (respectively, $(1 - z)E$) which fragments into a hadron h with energy xE .

tonic distributions inside a quark and gluon jet, $Q, G(z) = x/z D_{Q,G}^h(x/z, zE\Theta_0, Q_0)$, obey the system of two coupled

equations [6] (the subscript y denotes $\partial/\partial y$) following from the MLLA master equation described by (1)

$$Q_y = \int_0^1 dz \frac{\alpha_s}{\pi} \Phi_q^g(z) \left[(Q(1 - z) - Q) + G(z) \right], \quad (4)$$

$$G_y = \int_0^1 dz \frac{\alpha_s}{\pi} \left[\Phi_g^g(z)(1 - z)(G(z) + G(1 - z) - G) + n_f \Phi_g^q(z)(2Q(z) - G) \right]. \quad (5)$$

$\Phi_A^B(z)$ denotes the Dokshitzer-Gribov-Lipatov-Altarelli-Parisi (DGLAP) splitting functions [5],

$$\Phi_q^g(z) = C_F \left(\frac{2}{z} + \phi_q^g(z) \right), \quad \Phi_g^g(z)(1 - z) = 2N_c \left(\frac{1}{z} + \phi_g^g(z) \right), \\ \Phi_g^q(z) = T_R [z^2 + (1 - z)^2],$$

where $\phi_q^g(z) = z - 2$ and $\phi_g^g(z) = (z - 1)(2 - z(1 - z))$ are regular as $z \rightarrow 0$, $C_F = (N_c^2 - 1)/2N_c$, $T_R = n_f/2$ ($N_c = 3$ is the number of colors for $SU(3)_c$ and $n_f = 3$ is the number of light flavors we consider). The running coupling of QCD (α_s) is given by

$$\alpha_s = \frac{2\pi}{4N_c\beta_0(\ell + y + \lambda)}, \quad \beta_0 = \frac{1}{4N_c} \left(\frac{11}{3}N_c - \frac{4}{3}T_R \right)$$

and

$$\ell = (1/x), \quad y = \ln(k_\perp/Q_0), \quad \lambda = \ln(Q_0/\Lambda_{\text{QCD}}),$$

where Q_0 is the collinear cut-off parameter. Moreover,

$$G \equiv G(1) = x D_G^h(x, E\Theta_0, Q_0), \\ Q \equiv Q(1) = x D_Q^h(x, E\Theta_0, Q_0).$$

At small $x \ll z$, the fragmentation functions behave as

$$B(z) \approx \rho_B^h \left(\ln \frac{z}{x}, \ln \frac{zE\Theta_0}{Q_0} \right) = \rho_B^h(\ln z + \ell, y),$$

ρ_B^h being a slowly varying function of two logarithmic variables $\ln(z/x)$ and y that describes the ‘‘hump-backed’’ plateau. Since recoil effects should be largest in hard parton splittings, the strategy followed in this work is to perform Taylor expansions (first advocated for in [15]) of the non-singular parts of the integrands in (4,5) in powers of $\ln z$ and $\ln(1 - z)$, both considered small with respect to ℓ in the hard splitting region $z \sim 1 - z = \mathcal{O}(1)$

$$B(z) = B(1) + B_\ell(1) \ln z + \mathcal{O}(\ln^2 z); \quad z \leftrightarrow 1 - z. \quad (6)$$

Each ℓ -derivative giving an extra $\sqrt{\alpha_s}$ factor (see [6]), the terms $B_\ell(1) \ln z$ and $B_\ell(1) \ln(1 - z)$ yield NMLLA corrections to the solutions of (5). Making use of (6), after integrating over the regular parts of the DGLAP splitting functions, while keeping the singular terms unchanged, one gets after some algebra

$$(\gamma_0^2 = 2N_c\alpha_s/\pi) [9, 12]$$

$$Q(\ell, y) = \delta(\ell) + \frac{C_F}{N_c} \int_0^\ell d\ell' \int_0^y dy' \gamma_0^2(\ell' + y') \left[1 - \tilde{a}_1 \delta(\ell' - \ell) + \tilde{a}_2 \delta(\ell' - \ell) \psi_\ell(\ell', y') \right] G(\ell', y'), \quad (7)$$

$$G(\ell, y) = \delta(\ell) + \int_0^\ell d\ell' \int_0^y dy' \gamma_0^2(\ell' + y') \left[1 - a_1 \delta(\ell' - \ell) + a_2 \delta(\ell' - \ell) \psi_\ell(\ell', y') \right] G(\ell', y'), \quad (8)$$

with $\psi_\ell(\ell, y) = G_\ell(\ell, y)/G(\ell, y)$. The MLLA coefficients $\tilde{a}_1 = 3/4$ and $a_1 \approx 0.935$ are computed in [6] while at NM-LLA, we get

$$\tilde{a}_2 = \frac{7}{8} + \frac{C_F}{N_c} \left(\frac{5}{8} - \frac{\pi^2}{6} \right) \approx 0.42, \quad (9)$$

$$a_2 = \frac{67}{36} - \frac{\pi^2}{6} - \frac{13}{18} \frac{n_f T_R C_F}{N_c N_c} \approx 0.06. \quad (10)$$

Defining $F(\ell, y) = \gamma_0^2(\ell + y)G(\ell, y)$, we can exactly solve the self-contained equation (8) by performing the Mellin transform

$$F(\ell, y) = \iint \frac{d\omega d\nu}{(2\pi i)^2} e^{\omega\ell} e^{\nu y} \mathcal{F}(\omega, \nu). \quad (11)$$

Inserting (11) into (8) we obtain, after some algebra, the differential equation

$$\beta_0 \left(\lambda \mathcal{F} - \frac{\partial \mathcal{F}}{\partial \omega} - \frac{\partial \mathcal{F}}{\partial \nu} \right) = \frac{1}{\nu} + \frac{\mathcal{F}}{\omega\nu} - a_1 \frac{\mathcal{F}}{\nu} - a_2 \frac{\omega}{\nu} \mathcal{F}. \quad (12)$$

Finally, after inserting the solution of (12) into (11), the new integral representation for the inclusive spectrum (hump-backed plateau) with NMLLA accuracy reads

$$G(\ell, y) = (\ell + y + \lambda) \iint \frac{d\omega d\nu}{(2\pi i)^2} e^{\omega\ell} e^{\nu y} \int_0^\infty \frac{ds}{\nu + s} \times \left(\frac{\omega(\nu + s)}{(\omega + s)\nu} \right)^{\sigma_0} \left(\frac{\nu}{\nu + s} \right)^{\sigma_1 + \sigma_2} e^{-\sigma_3 s}, \quad (13)$$

where

$$\sigma_0 = \frac{1}{\beta_0(\omega - \nu)}, \quad \sigma_1 = \frac{a_1}{\beta_0}, \quad \sigma_2 = \frac{a_2}{\beta_0}(\omega - \nu), \quad \sigma_3 = \frac{a_2}{\beta_0} + \lambda.$$

However, computing (13) numerically is quite a challenging task. As can be seen, the NMLLA coefficient a_2 is very small. This may explain *a posteriori* why the MLLA “hump-backed plateau” agrees very well with experimental data [1, 14]. Therefore, the NMLLA solution (13) of (8) can be approximated by the MLLA solution of $G(\ell, y)$ (*i.e.* taking $a_2 \approx 0$), which will be used in the following to compute the inclusive k_\perp -distribution. As demonstrated in [6], taking the limits $a_2 \approx 0$ and $\lambda \approx 0$ in (13), the integral representation can be reduced to the known MLLA formula [5]

$$G(\ell, y) = 2 \frac{\Gamma(B)}{\beta_0} \int_0^{\frac{\pi}{2}} \frac{d\tau}{\pi} e^{-B\alpha} \mathcal{F}_B(\tau, y, \ell), \quad (14)$$

where the integration is performed with respect to τ defined by $\alpha = \frac{1}{2} \ln \frac{y}{\ell} + i\tau$ and with

$$\mathcal{F}_B(\tau, y, \ell) = \left[\frac{\cosh \alpha - \frac{y - \ell}{y + \ell} \sinh \alpha}{\frac{\ell + y}{\beta_0} \frac{\alpha}{\sinh \alpha}} \right]^{B/2} I_B(2\sqrt{Z(\tau, y, \ell)}),$$

$$Z(\tau, y, \ell) = \frac{\ell + y}{\beta_0} \frac{\alpha}{\sinh \alpha} \left(\cosh \alpha - \frac{y - \ell}{y + \ell} \sinh \alpha \right),$$

$B = a_1/\beta_0$ and I_B is the modified Bessel function of the first kind. To get a quantitative idea on the difference between MLLA and NMLLA gluon inclusive spectrum, the reader is reported to the appendix B of [9]. The magnitude of \tilde{a}_2 , however, indicates that the NMLLA corrections to the inclusive quark jet spectrum may not be negligible and should be taken into account. After solving (8), the solution of (7) reads

$$Q(\ell, y) = \frac{C_F}{N_c} \left[G(\ell, y) + (a_1 - \tilde{a}_1) G_\ell(\ell, y) + (a_1(a_1 - \tilde{a}_1) + \tilde{a}_2 - a_2) G_{\ell\ell}(\ell, y) \right] + \mathcal{O}(\gamma_0^2). \quad (15)$$

It differs from the MLLA expression given in [4] by the term proportional to $G_{\ell\ell}$, which can be deduced from the subtraction of $(C_F/N_c) \times (8)$ to Eq. (7).

3 Single inclusive k_\perp -distribution of charged hadrons in NMLLA

Computing the single inclusive k_\perp -distribution requires the definition of the jet axis. The starting point of our approach consists in considering the correlation between two particles (h1) and (h2) of energies E_1 and E_2 which form a relative angle Θ inside one jet of total opening angle $\Theta_0 > \Theta$ [16]. Weighting over the energy E_2 of particle (h2), this relation leads to the correlation between the particle (h=h1) and the energy flux, which we identify with the jet axis (see Fig. 2) [4]. Thus, the correlation and the relative transverse momentum k_\perp between (h1) and (h2) are replaced by the correlation, and transverse momentum of (h1) with respect to the direction of the energy flux. Finally, we obtain the double differential spectrum $d^2N/dx d\Theta$ of a hadron produced with energy $E_1 = xE$ at angle Θ (or $k_\perp \approx xE\Theta$) with respect to the jet axis. As demonstrated in [4], the correlation reads

$$\frac{d^2N}{dx d\ln \Theta} = \frac{d}{d\ln \Theta} F_{A_0}^h(x, \Theta, E, \Theta_0), \quad (16)$$

where $F_{A_0}^h$ is given by the convolution of two fragmentation functions

$$F_{A_0}^h \equiv \sum_{A=g,q} \int_x^1 du D_{A_0}^A(u, E\Theta_0, uE\Theta) D_A^h\left(\frac{x}{u}, uE\Theta, Q_0\right), \quad (17)$$

u being the energy fraction of the intermediate parton A . $D_{A_0}^A$ describes the probability to emit A with energy uE off the parton A_0 (which initiates the jet), taking into account the evolution of the jet between Θ_0 and Θ . D_A^h describes the probability to produce the hadron h off A with energy fraction x/u and transverse momentum $k_\perp \approx uE\Theta \geq Q_0$ (see Fig. 2). As dis-

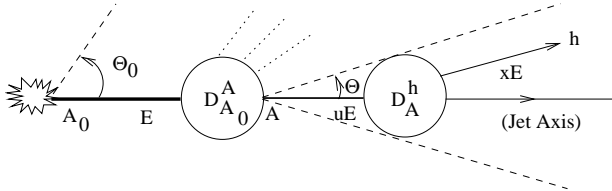


Figure 2. Inclusive production of hadron h at angle Θ inside a high energy jet of total opening angle Θ_0 and energy E .

cussed in [4], the convolution (17) is dominated by $u \sim 1$ and therefore $D_{A_0}^A(u, E\Theta_0, uE\Theta)$ is determined by the DGLAP evolution [5]. On the contrary, the distribution $D_A^h(\frac{x}{u}, uE\Theta, Q_0)$ at low $x \ll u$ reduces to the hump-backed plateau,

$$\tilde{D}_A^h(\ell + \ln u, y) \stackrel{x \ll u}{\approx} \rho_A^h(\ell + \ln u, Y_\Theta + \ln u), \quad (18)$$

with $Y_\Theta = \ell + y = \ln E\Theta/Q_0$. Performing the Taylor expansion of \tilde{D} to the second order in $(\ln u)$ and plugging it into Eq. (17) leads to

$$\begin{aligned} xF_{A_0}^h &\approx \sum_{A=g,q} \int du u D_{A_0}^A(u, E\Theta_0, uE\Theta) \tilde{D}_A^h(\ell, y) \\ &+ \sum_{A=g,q} \int du u \ln u D_{A_0}^A(u, E\Theta_0, uE\Theta) \frac{d\tilde{D}_A^h(\ell, y)}{d\ell} \\ &+ \frac{1}{2} \sum_{A=g,q} \left[\int du u \ln^2 u D_{A_0}^A(u, E\Theta_0, uE\Theta) \right] \frac{d^2 \tilde{D}_A^h(\ell, y)}{d\ell^2}. \end{aligned} \quad (19)$$

Indeed, since soft particles are less sensible to the energy balance, the correlation (17) is proved to disappear for these particles, leading to the sequence of factorized terms written in (19). The first two terms in Eq. (19) correspond to the MLLA distribution calculated in [4] when \tilde{D}_A^h is evaluated at NLO and its derivative at LO. NMLLA corrections arise from their respective calculation at NNLO and NLO, and, mainly in practice, from the third line, which was computed in [9, 12]. Indeed, since x/u is small, the inclusive spectrum $\tilde{D}_A^h(\ell, y)$ with $A = G, Q$ are given by the solutions (13) and (15) of the next-to-MLLA evolution equations (7) and (8) respectively. However, because of the smallness of the coefficient a_2 (see (10)), $G(\ell, y)$ shows no significant difference from MLLA to NMLLA. As a consequence, we use the MLLA expression (14) for $G(\ell, y)$, and the NMLLA (15) for $Q(\ell, y)$. The functions F_g^h and F_q^h are related to the gluon distribution *via* the color currents $\langle C \rangle_{g,q}$ defined as:

$$xF_{g,q}^h = \frac{\langle C \rangle_{g,q}}{N_c} G(\ell, y). \quad (20)$$

$\langle C \rangle_{g,q}$ can be seen as the average color charge carried by the parton A due to the DGLAP evolution from A_0 to A . Introducing the first and second logarithmic derivatives of \tilde{D}_A^h ,

$$\begin{aligned} \psi_{A,\ell}(\ell, y) &= \frac{1}{\tilde{D}_A^h(\ell, y)} \frac{d\tilde{D}_A^h(\ell, y)}{d\ell} = \mathcal{O}(\sqrt{\alpha_s}), \\ (\psi_{A,\ell}^2 + \psi_{A,\ell\ell})(\ell, y) &= \frac{1}{\tilde{D}_A^h(\ell, y)} \frac{d^2 \tilde{D}_A^h(\ell, y)}{d\ell^2} = \mathcal{O}(\alpha_s). \end{aligned}$$

Eq. (19) can now be written as

$$\begin{aligned} xF_{A_0}^h &\approx \sum_{A=g,q} \left[\langle u \rangle_{A_0}^A + \langle u \ln u \rangle_{A_0}^A \psi_{A,\ell}(\ell, y) \right. \\ &\left. + \frac{1}{2} \langle u \ln^2 u \rangle_{A_0}^A (\psi_{A,\ell}^2 + \psi_{A,\ell\ell})(\ell, y) \right] \tilde{D}_A^h, \end{aligned}$$

with the notation

$$\begin{aligned} \langle u \ln^i u \rangle_{A_0}^A &\equiv \int_0^1 du (u \ln^i u) D_{A_0}^A(u, E\Theta_0, uE\Theta) \\ &\approx \int_0^1 du (u \ln^i u) D_{A_0}^A(u, E\Theta_0, E\Theta). \end{aligned}$$

The scaling violation of the DGLAP fragmentation function neglected in the last approximation is a NMLLA correction to $\langle u \rangle$. It however never exceeds 5% [9] of the leading contribution and is thus neglected in the following. Using (20), the MLLA and NMLLA corrections to the leading color current of the parton $A_0 = g, q$ read

$$\delta \langle C \rangle_{A_0}^{\text{MLLA-LO}} = N_c \langle u \ln u \rangle_{A_0}^g \psi_{g,\ell} \quad (21)$$

$$\begin{aligned} &+ C_F \langle u \ln u \rangle_{A_0}^q \psi_{q,\ell}, \\ \delta \langle C \rangle_{A_0}^{\text{NMLLA-MLLA}} &= N_c \langle u \ln^2 u \rangle_{A_0}^g (\psi_{g,\ell}^2 + \psi_{g,\ell\ell}) \quad (22) \\ &+ C_F \langle u \ln^2 u \rangle_{A_0}^q (\psi_{q,\ell}^2 + \psi_{q,\ell\ell}). \end{aligned}$$

The MLLA correction, $\mathcal{O}(\sqrt{\alpha_s})$, was determined in [4] and the NMLLA contribution, $\mathcal{O}(\alpha_s)$, to the average color current is new. The latter can be obtained from the Mellin moments of the DGLAP fragmentation functions

$$\mathcal{D}_{A_0}^A(j, \xi) = \int_0^1 du u^{j-1} D_{A_0}^A(u, \xi),$$

leading to

$$\langle u \ln^2 u \rangle_{A_0}^A = \frac{d^2}{dj^2} \mathcal{D}_{A_0}^A(j, \xi(E\Theta_0) - \xi(E\Theta)) \Big|_{j=2}. \quad (23)$$

Plugging (23) into the resummed expression $\langle C \rangle_{g,q}$ of the color current as written in (20), these quantities for gluon and quark jets are determined analytically [9]. For illustrative purposes, the LO, MLLA, and NMLLA average color current of a quark jet with $Y_{\Theta_0} = 6.4$ – corresponding roughly to Tevatron energies – is plotted in Fig. 3 as a function of y , at fixed $\ell = 2$ for $\lambda \approx 0$. As discussed in [4], the MLLA corrections to the LO color current are found to be large and negative. As expected, the correction $\mathcal{O}(\alpha_s)$ from MLLA to NMLLA proves much

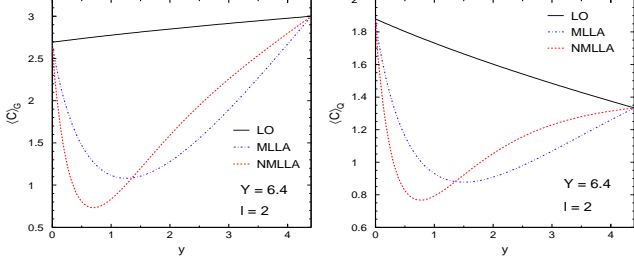


Figure 3. The color current of a gluon jet (left panel) and a quark jet (right panel) with $Y_{\Theta_0} = 6.4$ as a function of y at fixed $\ell = 2$ for $\lambda \approx 0$.

smaller; it is negative (positive) at small (large) y . This calculation has also been extended beyond the limiting spectrum, $\lambda \neq 0$, to take into account hadronization effects in the production of “massive” hadrons, $m = \mathcal{O}(Q_0)$ [18]. We used, accordingly, the more general MLLA solution of (8) with $a_2 = 0$ for an arbitrary $\lambda \neq 0$

$$G(\ell, y) = (\ell + y + \lambda) \iint \frac{d\omega d\nu}{(2\pi i)^2} e^{\omega\ell + \nu y} \int_0^\infty \frac{ds}{\nu + s} \times \left(\frac{\omega(\nu + s)}{(\omega + s)\nu} \right)^{1/\beta_0(\omega - \nu)} \left(\frac{\nu}{\nu + s} \right)^{a_1/\beta_0} e^{-\lambda s},$$

from which an analytic approximated expression was found using the steepest descent method [17]; $\sigma_2 = 0$ and $\sigma_3 = \lambda$ have been set in (13). However, $G(\ell, y)$ is here determined exactly from an equivalent representation in terms of a single Mellin transform (which reduces to (14) as $\lambda \rightarrow 0$) [18]

$$G(\ell, y) = \frac{\ell + y + \lambda}{\beta_0 B (B + 1)} \int_{\epsilon - i\infty}^{\epsilon + i\infty} \frac{d\omega}{2\pi i} e^{\omega\ell} \times \Phi(-A + B + 1, B + 2, -\omega(\ell + y + \lambda)) \mathcal{K}(\omega, \lambda) \quad (24)$$

which is better suited for numerical studies. The function \mathcal{K} appearing in Eq. (24) reads

$$\mathcal{K}(\omega, \lambda) = \frac{\Gamma(A)}{\Gamma(B)} (\omega \lambda)^B \Psi(A, B + 1, \omega \lambda), \quad (25)$$

where $A = 1/(\beta_0 \omega)$, $B = a_1/\beta_0$, and Φ and Ψ are the confluent hypergeometric function of the first and second kind, respectively. The NMLLA (normalized) corrections to the MLLA result are displayed in Fig. 4 for different values $\lambda = 0, 0.5, 1$, by using (24). It clearly indicates that the larger λ , the smaller the NMLLA corrections. In particular, they can be as large as 30% at the limiting spectrum ($\lambda = 0$) but no more than 10% for $\lambda = 0.5$. This is not surprising since $\lambda \neq 0$ ($Q_0 \neq \Lambda_{\text{QCD}}$) reduces the parton emission in the infrared sector and, thus, higher-order corrections. The double differential spectrum ($d^2N/d\ell dy$), Eq. (16), can now be determined from the NMLLA color currents (22) using the MLLA quark and gluon distributions. Integrating it over ℓ leads to the single inclusive y -distribution (or k_\perp -distribution) of hadrons inside a quark or a gluon jet:

$$\left(\frac{dN}{dy} \right)_{g,q} = \left(k_\perp \frac{dN}{dk_\perp} \right)_{g,q} = \int_{\ell_{\min}}^{Y_{\Theta_0} - y} d\ell \left(\frac{d^2N}{d\ell dy} \right)_{g,q}, \quad (26)$$

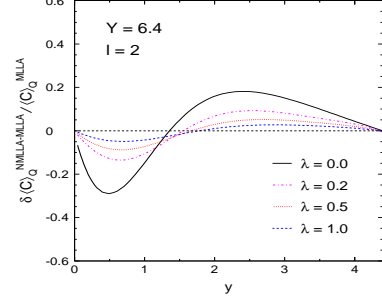


Figure 4. NMLLA corrections to the color current of a quark jet with $Y_{\Theta_0} = 6.4$ and $\ell = 2$ for various values of λ .

where

$$\left(\frac{d^2N}{d\ell dy} \right)_{A_0} = \frac{1}{N_c} \langle C \rangle_{A_0} \frac{d}{dy} G(\ell, y) + \frac{1}{N_c} G(\ell, y) \frac{d}{dy} \langle C \rangle_{A_0} \quad (27)$$

is the explicit expression of the double differential distribution (16). The MLLA framework does not specify down to which values of ℓ (up to which values of x) the double differential spectrum ($d^2N/d\ell dy$) should be integrated over. Since ($d^2N/d\ell dy$) becomes negative (non-physical) at small values of ℓ (see e.g. [4]), we chose the lower bound ℓ_{\min} so as to guarantee the positiveness of ($d^2N/d\ell dy$) over the whole $\ell_{\min} \leq \ell \leq Y_{\Theta_0}$ range (in practice, $\ell_{\min}^g \sim 1$ and $\ell_{\min}^q \sim 2$). Having successfully computed the single k_\perp -spectra including NMLLA corrections, we now compare the result with existing data. The CDF collaboration at the Tevatron recently reported on preliminary measurements over a wide range of jet hardness, $Q = E\Theta_0$, in $p\bar{p}$ collisions at $\sqrt{s} = 1.96$ TeV [13]. CDF data, including systematic errors, are plotted in Fig. 5 together with the MLLA predictions of [4] and the present NMLLA calculations, both at the limiting spectrum ($\lambda = 0$) and taking $\Lambda_{\text{QCD}} = 250$ MeV; the experimental distributions suffering from large normalization errors, data and theory are normalized to the same bin, $\ln(k_\perp/1 \text{ GeV}) = -0.1$. The agreement between the CDF results and the NMLLA distributions over the whole k_\perp -range is particularly good. In contrast, the MLLA predictions prove reliable in a much smaller k_\perp interval. At fixed jet hardness (and thus Y_{Θ_0}), NMLLA calculations prove accordingly trustable in a much larger x interval. Despite this encouraging agreement with data, the present calculation still suffers from certain theoretical uncertainties, discussed in detail in [9]. Among them, the variation of Λ_{QCD} –giving NMLLA corrections– from the default value $\Lambda_{\text{QCD}} = 250$ MeV to 150 MeV and 400 MeV affects the normalized k_\perp -distributions by roughly 20% in the largest $\ln(k_\perp/1 \text{ GeV}) = 3$ GeV-bin at $Q = 100$ GeV. Also, cutting the integral (26) at small values of ℓ is somewhat arbitrary. However, we checked that changing ℓ_{\min} from 1 to 1.5 modifies the NMLLA spectra at large k_\perp by $\sim 20\%$ only¹. Finally, the kt-distribution is determined with respect to the jet energy flow (which includes a summation over secondary hadrons in energy-energy correlations). In experiments, instead, the jet axis is determined exclusively from all particles inside the jet. The question of

¹ The effect of varying ℓ_{\min} is more dramatic at MLLA.

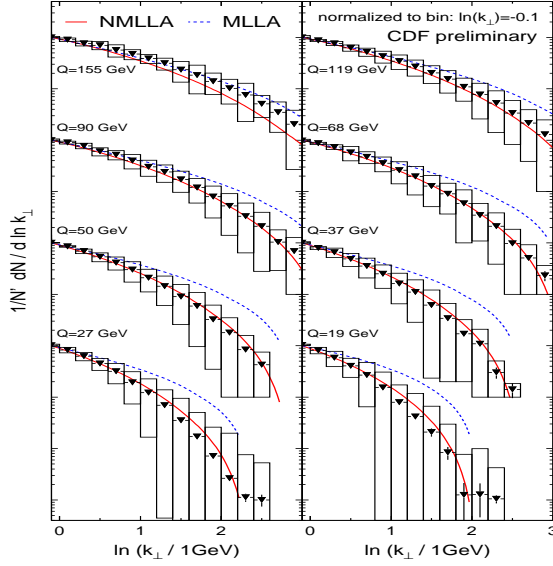


Figure 5. CDF preliminary results for the inclusive k_{\perp} distribution at various hardness Q in comparison to MLLA and NMLLA predictions at the limiting spectrum ($Q_0 = \Lambda_{QCD}$); the boxes are the systematic errors.

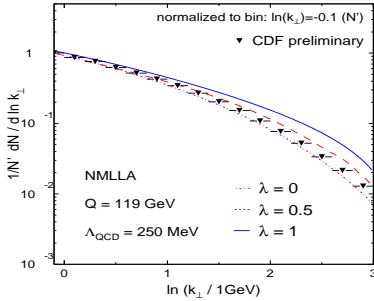


Figure 6. CDF preliminary results ($Q = 119$ GeV) for inclusive k_{\perp} distribution compared with NMLLA predictions beyond the limiting spectrum.

the matching of these two definitions goes beyond the scope of this letter. The NMLLA k_{\perp} -spectrum has also been calculated beyond the limiting spectrum, by plugging (24) into (26), as illustrated in Fig. 6. However, the best description of CDF preliminary data is reached at the limiting spectrum, or at least for small values of $\lambda \lesssim 0.5$, which is not too surprising since these inclusive measurements mostly involve pions. Identifying produced hadrons would offer the interesting possibility to check a dependence of the shape of k_{\perp} -distributions on the hadron species, such as the one predicted in Fig. 6. Moreover, the softening of the k_{\perp} -spectra with increasing hadron masses predicted in Fig. 6 is an observable worth to be measured, as this would provide an additional and independent check of the LPHD hypothesis beyond the limiting spectrum. This could only be achieved if the various species of hadrons inside a jet can be identified experimentally. Fortunately, it is likely to be the case at the LHC, where the ALICE [19] and CMS [20] experiments at the Large Hadron Collider have good identification capabilities at not too large transverse momenta.

4 Conclusion

To summarize, single inclusive k_{\perp} -spectra inside a jet are determined including higher-order $\mathcal{O}(\alpha_s)$ (i.e. NMLLA) corrections from the Taylor expansion of the MLLA evolution equations and beyond the limiting spectrum, $\lambda \neq 0$. The agreement between NMLLA predictions and CDF preliminary data in $p\bar{p}$ collisions at the Tevatron is impressive, indicating very small overall non-perturbative corrections and giving further support to LPHD [3]. The MLLA evolution equations for inclusive enough variables prove once more (see e.g. [5]) to include reliable information at higher orders than MLLA.

References

1. Yu.L. Dokshitzer, V.S. Fadin, V.A. Khoze, Phys. Lett. **B 115** (1982) 242;
Ya.I. Azimov, Yu.L. Dokshitzer, V.A. Khoze, S.I. Troian, Z. Phys. **C 31** (1986) 213;
C.P. Fong, B.R. Webber, Phys. Lett. **B 229** (1989) 289.
2. V.A. Khoze, W. Ochs, Int. J. Mod. Phys. **A 12** (1997) 2949.
3. Ya.I. Azimov, Yu.L. Dokshitzer, Z. Phys **C 27** (1985) 65;
Yu.L. Dokshitzer, V.A. Khoze, S.I. Troian, J. Phys. **G 17** (1991) 1585.
4. R. Pérez Ramos, B. Machet, JHEP **04** (2006) 043.
5. Yu.L. Dokshitzer, V.A. Khoze, A.H. Mueller, S.I. Troyan, (Editions Frontières, Gif-sur-Yvette, 1991).
6. R. Pérez Ramos, JHEP **06** (2006) 019 and references therein.
7. Yu.L. Dokshitzer, Phys. Lett. **B 305** (1993) 295.
8. F. Cuyper, K. Tesima, Z. Phys. **C 54** (1992) 87.
9. R. Perez-Ramos, F. Arleo & B. Machet, Phys. Rev. D **78** (2008) 014019.
10. V.A. Khoze, S. Lupia, W. Ochs, Phys. Lett. **B 386** (1996) 451.
11. DELPHI Collaboration: J. Abdallah *et al.*, Phys. Lett. **B 605** (2005) 37.
12. F. Arleo, R. Pérez-Ramos, B. Machet, Phys. Rev. Lett. **100** (2008) 052002.
13. S. Jindariani, A. Korytov & A. Pronko, CDF report CDF/ANAL/JET/PUBLIC/8406 (March 2007),
www-cdf.fnal.gov/physics/new/qcd/kt_distributions_06/cdf8406_Kt-jets_public.ps.
14. Yu.L. Dokshitzer, V.S. Fadin, V.A. Khoze, Z. Phys **C 18** (1983) 37.
15. I.M. Dremin, Phys. Usp. **37** (1994) 715;
ibid., Usp. Fiz. Nauk **164** (1994) 785;
I.M. Dremin, J.W. Gary, Phys. Rep. **349** (2001) 301;
I.M. Dremin, V.A. Nechitailo, Mod. Phys. Lett. **A9** (1994) 1471.
16. Yu.L. Dokshitzer, D.I. Dyakonov & S.I. Troyan, Phys. Rep. **58** (1980) 270.
17. R. Pérez Ramos, JHEP **09** (2006) 014.
18. Yu.L. Dokshitzer, V.A. Khoze, S.I. Troian, Z. Phys. **C 55** (1992) 107;
Yu.L. Dokshitzer, V.A. Khoze, S.I. Troian, Int. J. Mod. Phys. **A 7** (1992) 1875;
V.A. Khoze, W. Ochs, J. Wosieck, and references therein.
19. ALICE collaboration, J. Phys. **G32** (2006) 1295.
20. CMS collaboration, D. d'Enterria (Ed.) *et al.*, J. Phys. **G34** (2007) 2307.